5. A. A. Beg and A. S. Baldwin Jr., *Genes Dev.* **7**, 2064 (1993).
6. D. Thanos and T. Maniatis, *Cell* **80**, 529 (1995).
7. D. St. Johnston and C. Nüsslein-Volhard, *ibid.* **68**, 201 (1992).
8. R. Geisler, A. Bergmann, Y. Hiromi, C. Nüsslein-Volhard, *ibid.* **71**, 613 (1992); S. Kidd, *ibid.*, p. 623.
9. C. Hashimoto, K. L. Hudson, K. V. Anderson, *ibid.* **52**, 269 (1988).
10. D. S. Schneider, K. L. Hudson, T.-Y. Lin, K. V. Anderson, *Genes Dev.* **5**, 797 (1991); N. J. Gay and F. J. Keith, *Nature* **351**, 355 (1991); A. Heguy, C. T. Baldari, G. Macchia, J. L. Telford, M. Melli, *J. Biol. Chem.* **267**, 2605 (1992).
11. A. Letsou, S. Alexander, K. Orth, S. A. Wasserman, *Proc. Natl. Acad. Sci. U.S.A.* **88**, 810 (1991); C. A. Shelton and S. Wasserman, *Cell* **72**, 515 (1993).
12. G. E. Croston, Z. Cao, D. V. Goeddel, *J. Biol. Chem.* **270**, 16514 (1995).
13. We seeded 293 cells in 100-mm plates at a density of 30% and transfected them on the following day with IL-1RI expression plasmid (10 μg) (*12*) and pNeoSRαII (1 μg) containing the G418 resistance gene by the calcium phosphate precipitation method (*25*). Cells that stably incorporated transfected genes were selected with G418 (600 μg/ml) (Gibco). Ten individual colonies were cloned and expanded. IL-RI expression on the cell surface was determined by fluorescence-activated cell sorting (FACS) analysis with antibody to IL-1RI. Four clones that showed adequate levels of IL-1RI expression were adapted to suspension culture in CO_2-independent minimum essential medium (MEM, Mediatech) supplemented with 10% fetal bovine serum, glucose (4.5 g/ml), 1 mM sodium pyruvate (Gibco), streptomycin (100 μg/ml), and penicillin (100 μg/ml).
14. The 293 IL-1RI cells were sedimented at 500*g* for 5 min and resuspended in serum-free MEM medium (50×10^6 cells/ml). The cells were treated with recombinant human IL-1β (200 ng/ml, Genentech) for 3 min at 37°C and sedimented at 500*g* for 5 min at 4°C. All subsequent steps were done at 4°C. Cells were suspended in five volumes of lysis buffer [50 mM Hepes (pH 7.9), 250 mM NaCl, 5 mM dithiothreitol (DTT), 1 mM EDTA, 20 mM β-glycerophosphate, 5 mM *p*-nitrophenyl phosphate, 1 mM sodium orthovanadate, 1 mM benzamidine, 0.4 mM phenylmethylsulfonyl fluoride (PMSF), 1 mM sodium metabisulfite, leupeptin (10 μg/ml), aprotinin (10 μg/ml), 0.1% NP-40, and 10% (v/v) glycerol]. After incubation on ice for 30 min with occasional rocking, the cell lysate was centrifuged at 2000*g* for 10 min. Supernatants were collected and centrifuged at 125,000*g* for 2 hours. Supernatants were stored at −70°C.
15. First-dimensional electrophoresis was isoelectrofocusing. The tube gel preparation and running conditions were described previously [O'Farrell, *J. Biol. Chem.* **250**, 4007 (1975)]. A pH gradient was created with ampholines pH 5.0 to 7.0 and pH 3.5 to 9.5 (Pharmacia) blended at a ratio of 1:1. Second-dimensional separation was achieved with 7% SDS–polyacrylamide gel electrophoresis (SDS-PAGE).
16. After thawing, the extracts were centrifuged at 125,000*g* for 2 hours. Supernatants were incubated with 35 mg of rabbit immunoglobulin G (IgG) raised to IL-1RI (*12*) and protein A–Sepharose CL4B beads (25 ml) (Pharmacia) for 4 hours at 4°C with rocking. The beads were collected in a glass Econo-column (Bio-Rad), washed with 250 ml of wash buffer 1 [50 mM Hepes (pH 7.9), 250 mM NaCl, 5 mM DTT, 1 mM EDTA, 0.1% NP-40, 20 mM β-glycerophosphate, 1 mM sodium orthovanadate, 1 mM benzamidine, 0.4 mM PMSF, and 1 mM sodium metabisulfite], and resuspended in 50 ml of kinase buffer [20 mM tris-HCl (pH 7.6), 1 mM DTT, 20 mM $MgCl_2$, 20 mM β-glycerophosphate, 20 mM *p*-nitrophenyl phosphate, 1 mM EDTA, 1 mM sodium orthovanadate, 1 mM benzamidine, 0.4 mM PMSF, 1 mM sodium metabisulfite, 5 μM unlabeled ATP, and 100 μCi of [γ-^{32}P]ATP)]. The phosphorylation reaction was incubated at 30°C for 15 min and was then incubated with unlabeled ATP (100 μM) for 15 min. The protein A beads were collected and washed sequentially with 150 ml of wash buffer 1, 150 ml of wash buffer 2 [50 mM Hepes (pH 7.9), 1 M NaCl, 5 mM DTT, 1 mM EDTA, and 0.1% NP-40] and 150 ml of wash buffer 3 [50 mM Hepes (pH 7.9), 100 mM NaCl, 2 M urea, 5 mM DTT, 1 mM EDTA, and 0.1% NP-40)]. Proteins that remained bound were eluted with 50 ml of the elution buffer (buffer 3 with 7 M urea) overnight at 4°C with rocking. The eluted material was loaded onto a 0.5-ml Q Sepharose column. After they were washed extensively with the elution buffer, proteins bound (including pp100) were eluted with 1.5 ml of the elution buffer with 0.5 M NaCl. The eluate was concentrated in a Microcon 50 (Amicon) to 50 μl, diluted with 1 ml of isoelectrofocusing sample buffer (*15*), concentrated again to 50 μl, and then subjected to 2D gel electrophoresis.
17. J. Hou *et al.*, *Science* **265**, 1701 (1994).
18. S. Hanks and A. Quinn, *Methods Enzymol.* **200**, 38 (1991); S. Hanks and T. Hunter, *FASEB J.* **9**, 576 (1995).
19. T. Hirayama and A. Oka, *Plant Mol. Biol.* **20**, 653 (1992); T. V. Moran and J. C. Walker, *Biochim. Biophys. Acta* **1216**, 9 (1993).
20. G. B. Martin *et al.*, *Science* **262**, 1432 (1993).
21. Y. L. Ing, I. W. Leung, H. H. Heng, L. C. Tsui, N. J. Lassam, *Oncogene* **9**, 1745 (1994).
22. R. L. Galindo, D. N. Edwards, S. K. Gillespie, S. A. Wasserman, *Development* **121**, 2209 (1995).
23. The IRAK coding sequence was inserted in a bacterial T7 expression vector pRSETA (Invitrogen), in fusion with a sequence encoding a polyhistidine tag. Recombinant IRAK was made in *Escherichia coli* strain BL21 induced with 1 mM isopropyl-β-D-thiogalactopyranoside, and then purified under denaturing conditions on a nickel column (Qiagen). Purified protein was used for generating antibodies in rabbits (Zymed).
24. J. Großhans, A. Bergmann, P. Haffter, C. Nüsslein-Volhard, *Nature* **372**, 563 (1994).
25. F. M. Ausubel *et al.*, *Current Protocols in Molecular Biology* (Wiley, New York, 1994), p. 9.1.1.
26. A. P. Feinberg and B. Vogelstein, *Anal. Biochem.* **132**, 6 (1983).
27. Cells were collected by centrifugation in 5 ml of phosphate-buffered saline with 1 mM EDTA, washed once with medium (10 ml), sedimented, resuspended in 1 ml of medium, and transferred to 1.5-ml microtubes. IL-1β (200 ng/ml) was added to the tubes, followed by incubation at 37°C for the indicated time. The cells were collected by centrifugation and then lysed with 1 ml of lysis buffer (*14*). After incubation on ice for 30 min, the cell debris was sedimented in a microcentrifuge and discarded. The IL-1RI complexes were immunoprecipitated (*12*), resolved by SDS-PAGE, and transferred to nitrocellulose membrane, which were blotted with antiserum to IRAK.
28. We thank D. Goeddel and S. McKnight for inspiration, support, and scientific advice; S. Wasserman for pointing out the sequence similarity in the NH_2-terminal regions of IRAK and Pelle; A. Ashkenazi for providing IL-1RI expression plasmids; A. Bothwell for pNeoSRαII; K. Williamson for nucleotide sequencing; L. Xu and S. Wong for technical support; and V. Baichwal, M. Rothe, and U. Schindler for critical review of the manuscript.

4 October 1995; accepted 8 December 1995

TECHNICAL COMMENTS

How Much Solar Radiation Do Clouds Absorb?

Anomalous absorption of solar radiation by clouds is said to exist (*1*, *2*) because shortwave absorption inferred from solar flux measurements often exceeds theoretical prediction. R. D. Cess *et al.* (*3*) suggest that solar absorption in clouds is not only significantly larger than the model prediction, but also much larger than inferred by previous measurements, including those that originally suggested the anomaly.

Current understanding predicts that absorption of solar radiation by the entire atmospheric column containing clouds is only slightly enhanced over absorption by an equivalent clear sky column. Theory predicts that cloud absorption can exceed 20% of incoming radiation (*4*) and that this absorption occurs in place of rather than in addition to clear sky absorption. Significant absorption by cloud thus does not imply anomalous absorption, and the data collected in an aircraft in the study by Pilewskie and Valero (*5*, *6*), when averaged, is actually consistent with current understanding. Thus, neither report (*3*, *5*) indicates that cloud absorption (as opposed to the total column absorption) is actually enhanced.

Measurement of atmospheric absorption is difficult to make, as it requires measurement of all radiation flowing into and from a volume. In measurements made from aircraft (*3*, *5*), the volume is ill-defined, and measurement of fluxes on its boundaries is by necessity limited to just a few locations. The usual approach is to measure the fluxes at the cloud top and base along the flight line of the aircraft and to make assumptions about the representativeness of these measurements to the unsampled regions. Given these assumptions, absorption then results as a (usually small) residual of the differences in these fluxes. When error analyses of this approach is considered, the combination of undersampling of boundary fluxes and the natural variability of the real atmosphere is too great to produce credible results (*2*, *7*). This variability results in spuriously large positive and negative excursions-to-absorption calculated as a flux difference (*8*). Where the study by Cess *et al.* (*3*) differs from others is that the above-cloud flux data derive from satellite observations, whereas the surface measurements are obtained from either a single radiometer or a network of 11 radiometers. This analysis is supposed to account for large space and time scale variability and is supposed to accommodate undersampled boundary fluxes. The report (*3*) does not contain an error analysis and or evidence to support this assumption.

Cess *et al.* introduce an approach to the

analyses of these flux data [figure 1 in (3)] which expresses the fluxes at cloud top (represented as an albedo along the y axes) as a function of downward fluxes below cloud (expressed here as a transmittance along the x axis) (9). The slope β, they argue, is governed by absorption, and estimate its value to be -0.59, which is significantly different from a slope deduced by state-of-the-art radiative transfer models (10). Although the slopes characterizing the model results vary according to where clouds occur in the atmosphere [or more precisely, how much water vapor exists above clouds (4)], the relationships shown are similar to the model results quoted by Cess *et al.* (3). The purpose of the model results shown is not to highlight differences in the slope parameter β (as in Fig. 1), but to emphasize the implications for spectral albedo of the results of Cess *et al.* (as in Fig. 2). If their analyses are assumed to be correct, then it is unclear why our present understanding is so badly flawed and why other measurements are wrong.

The cloud absorption anomaly as posed by Cess *et al.* contradicts results from other data sets. Absorption of solar radiation in the troposphere including in clouds occurs largely in the near infrared (NIR) portion of the spectrum (4) (at wavelength λ longer than about 0.7 μm). If it is supposed that the enhancement occurs in the NIR region (11), then it is simple to estimate the magnitude of the change in NIR albedo (unlike absorption, reflection is a quantity that is measurable) that is required to produce the value β found by C95. This change (Fig. 2A) is a function of transmission and indicates that a reduction of radiation of 50 to 60% is needed to account for a value of β equal to -0.59 (cloud absorption in this case is more than doubled). Existing measurements of NIR albedo, a fundamentally more accurate measure than any residual estimates of absorption (2), do not support this kind of anomaly (Fig. 2B).

The reflection of NIR radiation from clouds is detected over a narrow band of wavelengths where absorption is small (but not negligible), that is, where the change in albedo (and absorption) must be greatest (in so-called windows) (Fig. 3, y axis). A corresponding reflection at visible wavelengths is where absorption is thought to be nonexistent (Fig. 3, x axis). The relation between these reflections depends on particle size (through particle size effects on absorption) and cloud optical thickness—a dependence successfully used to remotely sense cloud particle size (12). A 50% reduction of *nir* reflection leads to a change in the estimated particle size from 10 μm, typical of the droplet size if marine water clouds to 50 μm. This is consistent neither with the demonstrated capabilities of present cloud particle size retrievals nor with known microphysics of such clouds.

Without convincing error analyses, without a reproduction of the results using different analyses and different data, and without an explanation of why other published results are inconsistent with their own, then it is difficult to evaluate the findings of Cess *et al.* (3). The nonreproducible nature of their results (3) is suggested in the results of Nemesure *et al.* (13) who analyze the same Boulder tower data and arrive at a different conclusion about the effect of clouds on the shortwave forcing. The analyses of Pilewskie and Valero [see figures 6 and 7 in (5)] also conflicts with their own "direct" measurements of absorp-

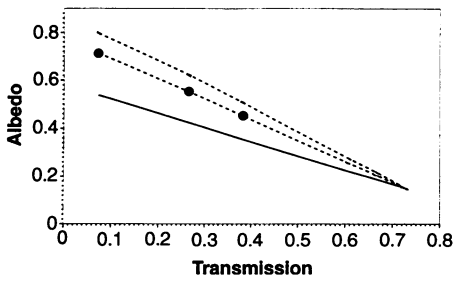

Fig. 1. Comparison of the albedo-transmission relation derived from state-of-the-art radiation models for high (---) and low (-•-) clouds contrasted to the relation shown in the report by Cess *et al.* (3). β = 0.59 (—). Units on the x and y axes are arbitrary.

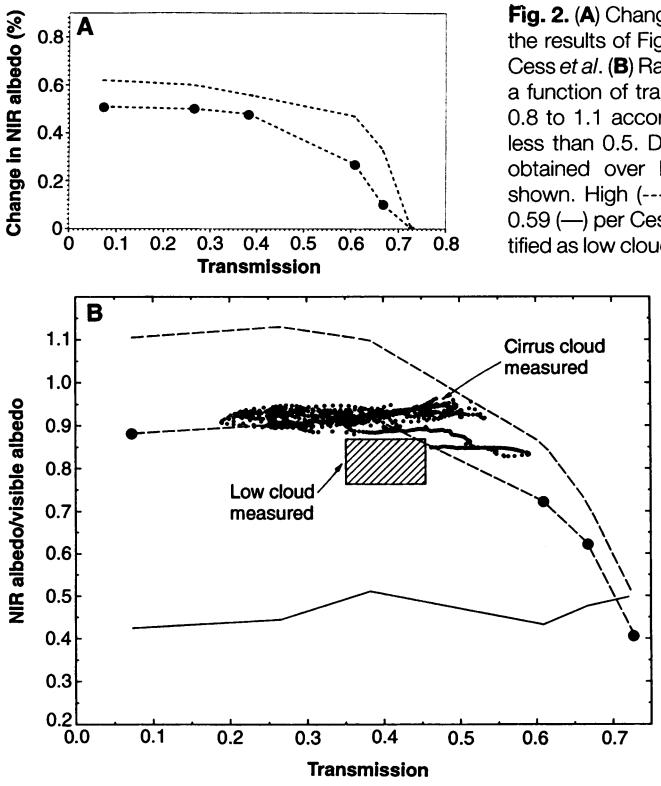

Fig. 2. (**A**) Change in NIR albedo required to bring the results of Fig. 1 into agreement with those of Cess *et al.* (**B**) Ratio of the NIR-to-visible albedo as a function of transmission. This ratio varies from 0.8 to 1.1 according to theory for transmissions less than 0.5. Direct measurements of this ratio obtained over low and high clouds are also shown. High (---) and low (-•-) clouds and β = 0.59 (—) per Cess *et al.* (3) are shown. Data identified as low cloud are from measurements reported by Hignett (12). Cirrus clouds measurements described by Smith *et al.* (13). Units on the x and y axes are arbitrary.

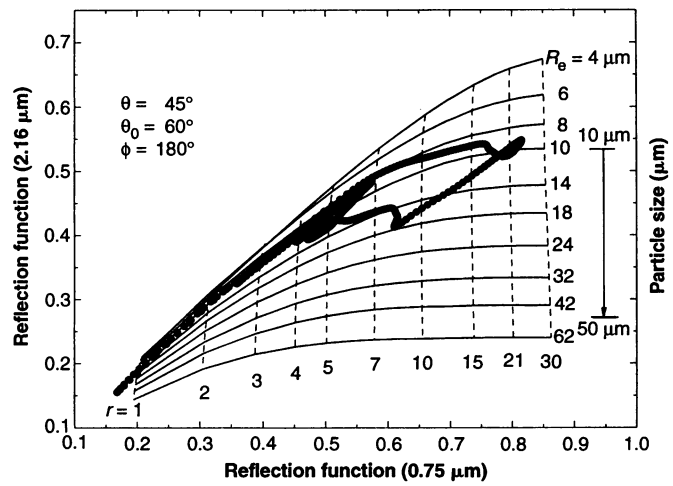

Fig. 3. NIR reflectance at 2.16 μm as a function of the 0.75 μm reflectance for a stratocumulus cloud from a 2-D radiative transfer model at a given solar-viewing geometry.

tion [figure 1 in (5)]. These results suggest that there are problems (7) with the indirect slope method used by Cess *et al.* (3). For example, the slope results in figure 6 in the report by Pilewskie and Valero (5) predicts that a cloud of 45% albedo absorbs in excess of 40% of the incident solar radiation, a result unsupported in their figure 1.

Graeme L. Stephens*
Cooperative Research Center for Southern Hemispheric Meteorology
Monash University,
Clayton, Victoria, Australia
E-mail: stephens@langley.atmos.colostate.edu

*Present address: Department of Atmospheric Science, Colorado State University, Fort Collins, CO 80523, USA.

REFERENCES AND NOTES

1. W. Wiscombe *et al.*, *J. Atmos. Sci.* **41**, 1336 (1984).
2. G. L. Stephens and S.-C. Tsay, *Q. J. R. Meteorol. Soc.* **116**, 671 (1990).
3. R. Cess *et al.*, *Science* **267**, 496 (1995).
4. G. L. Stephens, *J. Atmos. Sci.* **35**, 2111 (1978); S. Twomey, *ibid.* **33**, 1087 (1976); R. Davies *et al.*, *ibid.* **41**, 2126 (1984).
5. P. Pilewskie and F. Valero, *Science* **267**, 1626 (1995).
6. One can convert the flux difference measurements in the report by Pilewskie and Valero [figure 3 of (5)] to a fractional flux difference, which they would interpret as the fractional absorption. The mean values of the "absorption" would then range from approximately from 10% to 14%, which is entirely in keeping with theory. For reasons noted below (8), more significance should be attached to average values than to individual values [given in figure 2 of (5)].
7. This conclusion prompted other investigators to devise different ways of measuring absorption. An example is that of M. King *et al.* [*J. Atmos. Sci.* **47**, (1990)] who show slight discrepancies between theory and observation, but which is of a nature discussed by Stephens and Tsay (2) and does not support the results of Cess *et al.* (3).
8. T. Hayasaka *et al.*, *J. Appl. Meterol.* **34**, 1047 (1995). It is a typical practice to average the data in a effort to remove these spurious effects. Correction methods have also been developed, for example, by S. A. Ackerman and S. K. Cox [*ibid.* **20**, 1510 (1981)], to account for the spurious effects of undersampling solar fluxes around clouds. Correction methods were not used by Pilewskie and Valero (5).
9. A significant problem of the analyses by Cess *et al.* (3) is the assertion that reflection is a function of transmission. At absorbing wavelengths this assumption is wrong. The scattering and absorbing processes responsible for the measured albedo occur largely in the upper part of the cloud. Transmission depends on how these processes take place and not the other way around. It is more appropriate, at least on physical grounds, to consider transmission as a function of reflection (although even this is also not entirely correct). If the data of figure 6 of (5) are refitted with the dependent variables flipped, a slope of −0.82 results (which agrees with theory to the extent that the slope method is sensible). We use the model of Q. Fu and K. N. Lioa [*J. Atmos. Sci.* **50**, 2008 (1993)].
10. Theory predicts little solar absorption in the visible portion of the spectrum. Cess *et al.* imply that absorption of visible light by aerosol is unlikely to be the culprit, as they find similar anomalous values of β from flux data obtained in clean air masses over Cape Grim, Tasmania, Australia, where the relative cleanness of the air and its chemistry is well documented.
11. T. Nakajima *et al.*, *J. Atmos. Sci.* **48**, 728 (1991). There is a slight discrepancy between retrieved particle size and measured particle size. The retrieved particle sizes are typically a few microns larger than measured and explanation of the discrepancy has been elusive. It is, however, not close to the difference implied by the results of Cess *et al.* (3).
12. S. Nemesure *et al.*, *J. Climate* **7**, 579 (1994). D. Imre, personal communication.
13. P. Hignett, *Q. J. R. Meteorol. Soc.* **113**, 1011 (1987).
14. W. L. Smith Jr. *et al.*, *Mon. Weather Rev.* **118**, 2389 (1990).

5 May 1995; revised 8 May 1995; accepted 7 July 1995

Response: Stephens reflects a traditional viewpoint in stating that cloud "absorption occurs in place of rather than in addition to clear sky absorption." This is why theoretical cloud radiative transfer models predict roughly the same clear-sky and cloudy-sky (all-sky) solar absorption. But independent studies by Ramanathan *et al.* (1), Cess *et al.* (2), and Pilewskie and Valero (3) indicate that real clouds (or clouds plus atmosphere) absorb more solar radiation than do models. Stephens interprets the data in the report by Cess *et al.* (2) with the use of an atmospheric radiation model that adopts conventional plane-parallel clouds. He implements into this model a wavelength-dependent enhanced cloud absorption without adequate explanation; there are an infinite number of ways this calculation could be done, with probably infinite possible conclusions.

Stephens states that a "significant problem of the analysis by Cess *et al.* is the assertion that reflection is a function of transmission," which refers to the albedo versus transmittance regression. But as was demonstrated (2) for the Boulder-GOES data (obtained from the Geostationary Operational Environmental Satellite), the regression analysis was consistent with a direct determination of shortwave (SW) cloud-radiative forcing at the surface, $C_s(S)$, and at the top of the atmosphere, $C_s(TOA)$. This produced $C_s(S)/C_s(TOA) = 1.46$, a value that is in agreement with 1.41 from the regression analysis. Similar $C_s(S)/C_s(TOA)$ values were obtained in the other studies (1–3). In contrast, theoretical models produce $C_s(S)/C_s(TOA) \approx 1$, and this difference can only be explained by the models underestimating cloudy-sky absorption relative to clear-sky absorption (1–3).

Cess *et al.* (2) adopted the regression analysis for two reasons. First, only surface insolation was available at the other sites so it was not possible to directly determine $C_s(S)$. Second, the regression analysis did not require clear-sky identification of the surface measurements, which was difficult to determine for some data. But it is a simple task to demonstrate [in a manner analogous to what was done for the Boulder-GOES data, and using data for which we can confidently identify clear surface measurements (4)] that the regression analysis is consistent with an alternate treatment of TOA and surface measurements. With α denoting the TOA albedo and T the atmospheric transmittance (surface insolation divided by TOA insolation), it is straightforward to show that

$$\Delta\alpha/\Delta T = -(N-N_c)/(I-I_c) \quad (1)$$

where N is the net downward SW radiation at the TOA, I is the surface insolation, and N_c and I_c refer to clear-sky conditions. One can compare $\Delta\alpha/\Delta T$ (Fig. 1) as evaluated from regressions to that determined from Eq. (1), which addresses the issue of temporal and spatial sampling errors raised by Stephens. Equation 1 requires only that such errors be random so that they average to zero when evaluating the numerator and denominator of Eq. 1. The α versus T regression, however, explicitly requires all errors to be in the satellite measurements; if they were in the surface measurements, then a T versus α regression would be required, and $\Delta\alpha/\Delta T$ would be increased by the factor $1/R^2$, where R is the correlation coefficient. Sampling errors are attributable to the satellite measurements as demonstrated by the agreement between Eq. 1 and $\Delta\alpha/\Delta T$ as evaluated from the α versus T regression (Fig. 1). If it were more appropriate, as Stephens suggests, to consider T as a function of α, then Eq. 1 should agree with $\Delta\alpha/\Delta T$ as determined from the T versus α regression. This is not the case (Fig. 1), except for Oklahoma, where the large R makes the choice of the regression immaterial.

The reason that sampling errors are not attributable to the surface measurements is partially a result of temporal averaging of the surface measurements. Sampling errors occur because the satellite pixel measurements are instantaneous and over a grid that is much larger than the field of view of an upward facing pyranometer. For example, a single isolated cloud could significantly impact the surface measurement while having little impact on the satellite measurement; the reverse would occur if there were clouds over most of the satellite grid, but not over the surface instrument. But cloud systems move, so that temporally averaging the surface measurements is equivalent to spatially averaging them over the satellite grid. The Oklahoma data demonstrate this point: The regression R

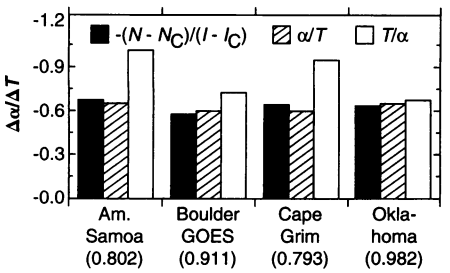

Fig. 1. $\Delta\alpha/\Delta T$ determined from Eq. 1, from an α versus T regression, and from a T versus α regression, for four geographically diverse locations. Correlation coefficients are indicated at bottom.

How Much Solar Radiation Do Clouds Absorb?

G. L. Stephens, R. D. Cess, M. H. Zhang, P. Pilewskie and F. P. J. Valero

Science **271** (5252), 1131.
DOI: 10.1126/science.271.5252.1131